Steady-State and Dynamic Properties of Cardiac Sodium-Calcium Exchange

Sodium-dependent Inactivation

DONALD W. HILGEMANN, SATOSHI MATSUOKA, GEORG A. NAGEL, and ANTHONY COLLINS

From the Department of Physiology, University of Texas Southwestern Medical Center at Dallas, Dallas, Texas 75235; and the Laboratory of Cardiac/Membrane Physiology, Rockefeller University, New York 10021

ABSTRACT Sodium-calcium exchange current was isolated in inside-out patches excised from guinea pig ventricular cells using the giant patch method. The outward exchange current decayed exponentially upon activation by cytoplasmic sodium (sodium-dependent inactivation). The kinetics and mechanism of the inactivation were studied. (*a*) The rate of inactivation and the peak current amplitude were both strongly temperature dependent (Q_{10} = 2.2). (*b*) An increase in cytoplasmic pH from 6.8 to 7.8 attenuated the current decay and shifted the apparent dissociation constant (K_d) of cytoplasmic calcium for secondary activation of the exchange current from 9.6 μM to <0.3 μM. (*c*) The amplitude of exchange current decreased synchronously over the membrane potential range from −120 to 60 mV during the inactivation, indicating that voltage dependence of the exchanger did not change during the inactivation process. The voltage dependence of exchange current also did not change during secondary modulation by cytoplasmic calcium and activation by chymotrypsin. (*d*) In the presence of 150 mM extracellular sodium and 2 mM extracellular calcium, outward exchange current decayed similarly upon application of cytoplasmic sodium. Upon removal of cytoplasmic sodium in the presence of 2–5 μM cytoplasmic free calcium, the inward exchange current developed in two phases, a fast phase within the time course of solution changes, and a slow phase ($\tau \approx 4$ s) indicative of recovery from sodium-dependent inactivation. (*e*) Under *zero-trans* conditions, the inward current was fully activated within solution switch times upon application of cytoplasmic calcium and did not decay. (*f*) The slow recovery phase of inward current upon removal of cytoplasmic sodium was also present under the *zero-trans* condition. (*g*) Sodium-dependent inactivation shows little or no dependence on membrane potential in guinea pig myocyte sarcolemma. (*h*) Sodium-dependent inactivation of outward current is attenuated in rate and extent as extracellular calcium is decreased. (*i*) Kinetics of the sodium-dependent inactivation and its dependence on major experimental vari-

Address reprint requests to Donald W. Hilgemann, Department of Physiology, University of Texas Southwestern Medical Center at Dallas, 5323 Harry Hines Boulevard, Dallas, TX 75235.

J. GEN. PHYSIOL. © The Rockefeller University Press · 0022-1295/92/12/0905/28 $2.00
Volume 100 December 1992 905–932

ables are well described by a simple two-state inactivation model assuming one fully active and one fully inactive exchanger state, whereby the transition to the inactive state takes place from a fully sodium-loaded exchanger conformation with cytoplasmic orientation of binding sites ($E_1 \cdot 3N_i$).

INTRODUCTION

It is well established that ion channels fluctuate between fully conducting and nonconducting states (e.g., Hille, 1992). To what extent other ion-transporting proteins might oscillate between functionally active and inactive states is not established. For the cardiac sodium-calcium exchanger (for overview of recent work see Blaustein, DiPolo, and Reeves, 1991), work with giant excised membrane patches suggests that a Markovian analysis, assuming the existence of active and inactive states, might well be useful (Hilgemann, Collins, Cash, and Nagel, 1991*a*). The outward exchange current ("calcium influx exchange mode") evidently inactivates in response to an increase of cytoplasmic sodium on a time scale of seconds. Experimental tests for ion concentration changes as a cause of these transients have been negative, and the kinetics are much too slow to reflect pre–steady-state transients of the exchange cycle itself (Hilgemann, 1990). Cytoplasmic calcium (Hilgemann, 1990), MgATP (Hilgemann, 1990; Collins, Somlyo, and Hilgemann, 1992), and phosphatidylserine (Hilgemann and Collins, 1992) all activate the exchanger by decreasing the extent of sodium-dependent inactivation. The secondary modulatory processes coupled to sodium-dependent inactivation can be functionally removed by limited proteolysis from the cytoplasmic side, leaving the exchanger in a highly stimulated state (Hilgemann, 1990). Accordingly, it appears that catalytic (transport) activity of the exchanger is regulated by a cytoplasmic autoinhibitory domain of the exchanger or an auxiliary inhibitory protein, similar in a general sense to the inactivation of some channels (Hille, 1992) and to the calmodulin-dependent regulation of the plasmalemmal Ca-ATPase (Carafoli, 1991).

With this background, we have begun analysis of the secondary kinetic properties of cardiac sodium-calcium exchange. Here, we describe kinetics of the sodium-dependent inactivation process, the recovery from inactivation, and effects of major experimental variables. We demonstrate that both calcium influx and calcium efflux modes of exchange are affected by the inactivation process and demonstrate its relevance to inward exchange current. We pinpoint the likely entrance point into inactivation as being a conformation with fully loaded sodium binding sites oriented to the cytoplasmic side. Simulations of a simple two-state inactivation reaction scheme allow reconstructions of most experimental results.

METHODS

Preparation of Single Myocytes

Myocytes were isolated from guinea pig ventricles as previously described (Collins et al., 1992). In brief, guinea pigs were anesthetized by intraperitoneal injection of pentobarbital sodium. Hearts were then rapidly removed and transferred to a Langendorff-type perfusion apparatus. Myocytes were isolated by retrograde perfusion of the hearts with nominally calcium-free solution containing collagenase (type B, 0.25 mg/ml; Boehringer Mannheim Corp., Indianap-

olis, IN, and type 2, 0.25 mg/ml; Worthington Biochemical Corp., Freehold, NJ) at 37°C. Digested tissue segments were placed in a "storage solution" (Collins et al., 1992) for 8–48 h at 4°C to induce the formation of large membrane blebs.

Electrophysiology

The giant patch method was used as described previously for cardiac myocytes (Hilgemann, 1989; Collins et al., 1992). Except as described in words, all results are with patches from guinea pig myocytes at 34–36°C. The patch clamp (Axopatch 1D) was controlled by a custom-built pulse generator (Victor Cordoba, UCLA, Los Angeles, CA), signals were acquired at 1–20 kHz (DT2831; Data Translation, Marlboro, MA), and subsequent processing was performed with our own software.

Solutions

The standard superfusion solutions employed were similar to cytoplasmic solutions used previously (Hilgemann, 1989; Collins et al., 1992). Pipette solutions were chosen to allow

TABLE I

Primary Experimental Solutions

	Standard superfusion solution	Pipette solution A	Pipette solution B	Pipette solution C
EGTA	9 mM	20 μM	20 μM	10 mM
$CaCl_2$	0–10 mM	4 mM	1 mM	—
(Na + Cs)-MES	100 mM	—	—	—
NMG-MES	—	100 mM	—	—
Na-MES	—	—	140 mM	140 mM
LiCl or KCl	—	10 mM	10 mM	—
$MgCl_2$	1 mM	2 mM	2 mM	4 mM
TEA-MES	18 mM	20 mM	20 mM	20 mM
Cs-MES	18 mM	20 mM	20 mM	20 mM
HEPES	25 mM	10 mM	10 mM	10 mM
Ouabain	—	200 μM	200 μM	200 μM
Verapamil	—	2 μM	2 μM	2 μM
$BaCl_2$	—	0.5 mM	0.5 mM	—
pH	7.0	7.0	7.0	7.0

recording of isolated outward exchange current, inward current, or mixed currents, depending on the cytoplasmic solutions used (Table I). Modifications of these solutions for individual experiments are given in the text and figure legends. Dibromo-BAPTA was prepared as a cesium salt by Molecular Probes, Inc. (Eugene, OR).

Controls for Isolation of Sodium-Calcium Exchange Current

Outward exchange currents were isolated in the presence of extracellular calcium and in the absence of extracellular sodium (i.e., in the pipette) by subtracting currents in the absence of cytoplasmic sodium from currents in the presence of cytoplasmic sodium. Controls for effects of cytoplasmic solutions on background conductances were performed with magnesium rather than calcium in the pipette solution. Inward exchange currents were determined in the presence of extracellular sodium and the absence of extracellular calcium by subtracting

currents in the absence of cytoplasmic calcium from currents in the presence of cytoplasmic calcium.

In preliminary studies, the possible existence of background sodium conductance was investigated by replacing cytoplasmic sodium with cesium in the absence of extracellular sodium (substituted by 140 mM cesium) and calcium. No significant difference in membrane current was found over a wide range of membrane potentials examined. Therefore, background sodium conductance is considered to be negligible in giant patches under the conditions of our exchange current measurements. Background calcium conductances and calcium-activated conductances were also negligible up to ~64 μM cytoplasmic free calcium when 150 mM lithium, NMG, or cesium was substituted for sodium in the pipette (see Fig. 3). At higher cytoplasmic calcium concentrations, calcium sometimes increased background conductance, perhaps via the calcium-activated nonselective cation channels (Ehara, Noma, and Ono, 1988). We cannot be confident about this interpretation because high cytoplasmic calcium concentrations had very variable and sometimes irreversible effects, including patch disruption. These results are consistent with a perturbation of the patch seal rather than a specific channel-mediated conductance. In individual cases in which "nonspecific" current was found, the current tended to run down and the amplitude of the current was much smaller than the exchange current. For these reasons, we are confident that contamination by calcium-activated nonspecific conductances is negligible in records shown for the inward exchange current and for the outward current in the presence of cytoplasmic calcium.

In the experiments with mixed inward and outward currents, the pipette solution contained 150 mM sodium and 2 mM calcium. The exchange currents were isolated as a difference current between currents activated by cytoplasmic sodium and/or calcium and those in the absence of both those ions.

It is noted as a caution that we also rigorously tested other possible means to isolate the exchange current. First, divalent cations other than calcium or magnesium were tested on current–voltage (*I-V*) relations in the absence of sodium and calcium. Clearly, the leak pathway and/or genuine background conductances of the membrane were blocked by both nickel and cobalt in the same concentration range (0.5–3 mM) needed to block exchange current from the cytoplasmic side. This virtually precludes their use to determine the exchange current. As another alternative, we tested dichlorobenzamil. Over exactly the same concentration range that blocked the isolated inward and outward exchange currents (0.5–10 μM), dichlorobenzamil also potently blocked the leak current components. Accordingly, we conclude that dichlorobenzamil has no specificity at all with respect to the exchange current and cannot be used to define the current or current transients associated with the exchanger in giant patches. It was notable that we found complete block of inward exchange current by 10–20 μM dichlorobenzamil from the cytoplasmic side. This is different from the results of Niggli and Lederer (1991), who reported no block of inward exchange current by up to 1 mM dichlorobenzamil applied from the pipette in whole myocyte experiments.

In one series of experiments, the possible chloride ion dependence of the exchanger and/or contamination of chloride conductance were estimated. 25 mM malic acid (Sigma Chemical Co., St. Louis, MO) was used as a calcium buffer in the pipette solution, and further, chloride ions in both pipette and cytoplasmic solutions were replaced with appropriate substitutes. In such experiments, composition of the pipette solution was (mM): 100 methanesulfonic acid (Sigma Chemical Co.), 25 malic acid, 2 $Mg(OH)_2$, 0.4–20 $CaCO_3$, 10 HEPES, 140 NMG, 10 CsOH, 0.01 verapamil, and 0.25 ouabain, pH 7.0 adjusted with methanesulfonic acid. Free calcium concentrations in pipette solutions were measured with tetramethylmurexide by spectrophotometry (Hilgemann, Delay, and Langer, 1983). Composition of the cytoplasmic solution (mM): 100 methanesulfonic acid, 10 EGTA, 1 $Mg(OH)_2$, 20 HEPES, 20 TEA-OH, 20

CsOH, and 100 CsOH or NaOH. 7.5 mM $CaCO_3$ was added to solutions to give 1 μM free calcium, pH 7.0 with methanesulfonic acid. Typical current traces and *I-V* relations under this condition are shown in Fig. 6 of an accompanying article (Matsuoka and Hilgemann, 1992). No remarkable differences in sodium-dependent inactivation and voltage dependence were found for the outward exchange current, with or without chloride ions and malic acid.

As a final methodological issue related to isolation of the exchange current, arguments are summarized that speak against a possibility that the exchange current transients interpreted as sodium-dependent inactivation are caused by ion concentration changes on either membrane side in the giant patches. (*a*) The current transients are unchanged when free calcium concentrations on both membrane sides are very heavily buffered or when the buffer capacity on the cytoplasmic side is substantially reduced (Hilgemann, 1990). (*b*) The inclusion of sodium in the pipette at a concentration of 50 mM (Hilgemann, 1990) or even 150 mM, as described in Fig. 9, does not change the pattern of current transients, which would have been the case if extracellular sodium accumulation were involved. (*c*) The expected magnitudes of ion concentration changes at membrane surfaces for the flux densities occurring in these experiments, assuming simple patch membrane geometry and a three-to-one sodium-calcium exchange stoichiometry, are in the range of a few micromolar to tens of micromolar (unpublished simulations). (*d*) Experimentally, we have attempted to estimate the magnitude of ion concentration changes that can take place in the pipette tip. To do so, inward exchange current was activated by a high cytoplasmic free calcium concentration (50 μm) in the presence of 150 mM extracellular sodium and in the absence of both calcium and EGTA on the extracellular side (i.e., in the pipette). When the calcium-containing cytoplasmic solution (50 μM free calcium) was switched to a calcium-free, 100 mM sodium-containing cytoplasmic solution, a small outward current transient could be detected. The transient decayed within 5 s, and it was obtained whether or not the exchanger had been "deregulated" with chymotrypsin. Based on our knowledge of the ion dependencies of exchange currents under these conditions, the accumulation of calcium in the pipette tip, induced by the fully activated inward exchange current, was estimated to be 50 μM.

Concentration–Current Relations

Concentration–current relations were measured so as to minimize a skewing of results by time-dependent current changes (run-down) and shifts of current baseline. The procedure is described in Fig. 1 for inward exchange current (pipette solution C, 140 mM extracellular sodium and no calcium, sodium-free cytoplasmic solution). A nearly maximal concentration of cytoplasmic calcium was applied. The cytoplasmic calcium concentration was then decreased in stepwise fashion as indicated, and again increased similarly in steps. Exchange current magnitudes were determined as the difference current between current values at the different calcium concentrations and a baseline current drawn between current values obtained in the absence of calcium before and after a concentration run. Values presented are averages of the values from the descending and ascending relationships.

Current–Voltage Relations

Fig. 2 demonstrates the method used to determine *I-V* relations of the exchange current. Fig. 2*A* is a typical record of outward exchange current (pipette solution A) at 0 mV. Upon substitution of 100 mM cesium in the cytoplasmic (bathing) solution for 100 mM sodium, an outward current of ~50 pA was activated. It decayed by ~80% over 10 s. Subsequently, as indicated, sodium was removed in replacement for cesium. At the spikes in the current record marked *a* (during sodium application) and *b* (after sodium application), the voltage protocol

described in Fig. 2 *B* was applied. As indicated in the lower part of *B*, voltage was changed in 20-mV steps from 0 to −120 mV, up to +60 mV, and back to 0 mV. Step duration was either 25 ms (as here) or 10 ms, and the mean current magnitude was determined over a 3-ms period at the end of the step. Time-dependent current changes have not been observed after decay of the capacitive current. Although fast sodium channels exist in the giant cardiac patch membrane (Hilgemann, 1989), sodium current was not activated by the pulse protocol used. It is noted in this regard that the sodium current undergoes slow inactivation in giant patches and that steady-state inactivation is shifted in the hyperpolarizing direction in giant patches (Collins, A., and D. W. Hilgemann, unpublished observations).

The data points were then plotted in X-Y format, as shown in Fig. 2 *C*, and were connected by lines. To obtain the *I-V* relation of the putative exchange current, the record *b* in the presence of cesium was subtracted from that in sodium (*a*) as the best estimate of the outward exchange current (open circles, $a - b$). Note that there is no hysteresis in the *I-V* relation

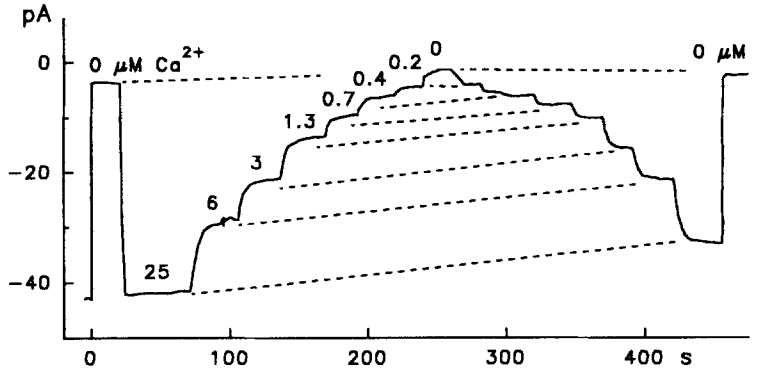

FIGURE 1. Procedure for determining cytoplasmic free calcium concentration–inward exchange current relations. Pipette solution C. Free calcium was stepped to the indicated concentrations by sequentially superfusing the appropriate solutions through the same inlet line (i.e., slow solution changes), except for the first activation. For evaluation of the concentration–current relation, a baseline in zero calcium was drawn, and the final current values obtained during superfusion at a given calcium concentration were averaged from the descending and ascending records.

during this protocol. Finally, a smoothing function (solid curve) was fitted to the data points by a least-squares method. Under most conditions studied to date, we find that the following equation satisfactorily describes the wave-form of individual sodium-calcium exchange *I-V* relationships:

$$I = (a \times K_{em} - b/K_{em})/(1 + c \times K_{em} + d/K_{em}) \quad (1)$$

where K_{em} is $e^{(Em \cdot F/2RT)}$, Em is membrane potential, and a, b, c, and d are constants. F, R, and T have their usual meanings. For isolated outward exchange current the b and d variables were eliminated; for isolated inward exchange current the a and c variables were eliminated. Although the general form of this equation arises in the solution of simple transport models (e.g., Stein, 1986; Läuger, 1991), no special meaning is attached to the constants. As appropriate for *I-V* relations of mixed outward and inward exchange current, the equation can be used to determine independently the reversal potentials in an accompanying article

(Matsuoka and Hilgemann, 1992). In the context of this article, the equation is used only as an independent test for changes of *I-V* wave form.

Intrapipette Perfusion in Excised Patches

The intrapipette perfusion technique of Soejima and Noma (1984) was used to study extracellular ion dependencies of the exchange current in inside-out patches. Fig. 3 demonstrates the time course of perfusion of the pipette solution and diffusion to the extracellular membrane surface. With pipette solution C (150 mM Na-MES), inward exchange currents were

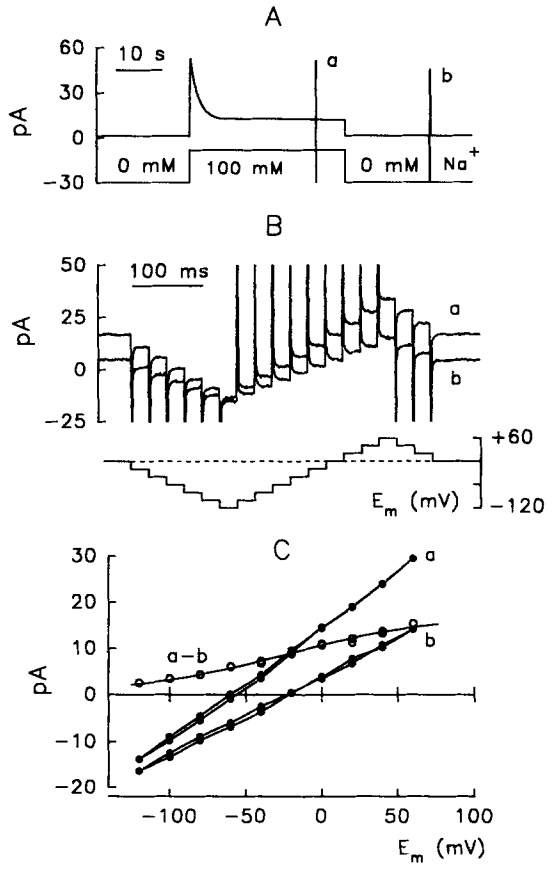

FIGURE 2. Measurement of *I-V* relations of the exchange current. (*A*) Chart record of membrane current; 2 μM cytoplasmic calcium and 8 mM extracellular calcium. Outward exchange current was activated by a rapid replacement of 100 mM cytoplasmic cesium with 100 mM sodium as indicated below the current record. *I-V* relations were measured during (*a*) and after (*b*) the application of sodium. (*B*) Membrane currents in response to membrane potential changes at *a* and *b* in panel *A*. The membrane potential protocol is given below the current records. (*C*) *I-V* relations of the currents at *a* and *b*. Mean current amplitudes were measured over 3 ms at the end of the step and plotted against membrane potential. The *I-V* relation of the outward exchange current was determined as the difference between *a* and *b* (*a* − *b*). See text for the smoothing function used and further details.

activated by step increments of cytoplasmic free calcium from 0 to 20 μM. The pipette perfusion started at the point indicated above the current trace and extracellular sodium was replaced with equimolar NMG. The inward current disappeared within ~1 min (usually 1–2 min) and application of cytoplasmic calcium then failed to evoke inward current, indicating complete replacement of extracellular sodium. Reperfusion of pipette solution with sodium-containing solution again activated inward current, demonstrated to be exchange current by step applications of cytoplasmic calcium. In the course of the experiment, the amplitude of the inward current decreased and zero current level shifted with time.

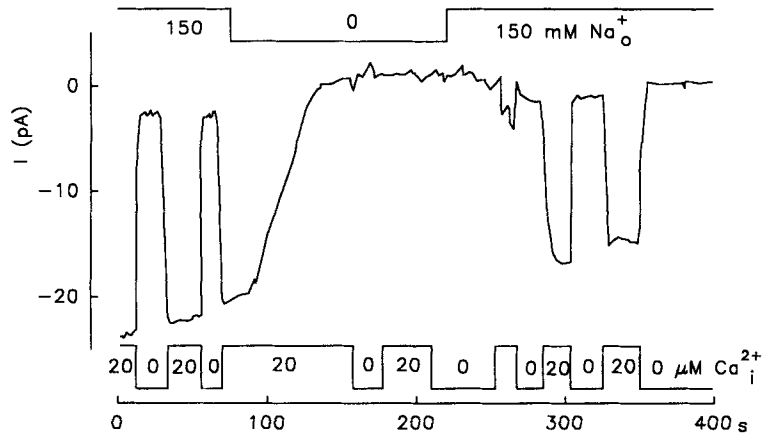

FIGURE 3. Inward sodium-calcium exchange current with pipette perfusion. The exchange current was activated by cytoplasmic calcium as indicated below the current record. 150 mM extracellular sodium, 0 extracellular calcium, and 0 cytoplasmic sodium. Extracellular sodium was then removed and again applied with the intrapipette perfusion method as indicated above the current record. Note complete loss of calcium-activated current in the absence of extracellular sodium.

Data Fitting

Ion dependencies of the exchange currents were fit by a least-squares method to applicable equations multiplied by a scaler variable. The Hill equation employed was:

$$\delta I = \delta I_{max} \times X^n/(X^n + K_h^n) \tag{2}$$

where δI is the measured change of current from a measured baseline, δI_{max} is a fitted maximum change of current, X is the concentration of the ion varied, K_h is the fitted half-effective concentration of X, and n is the fitted slope coefficient.

For the experiments in which inhibition of exchange current by an ion was examined, a modified Hill equation was used:

$$\delta I = \delta I_{max} \times K_i^n/(X^n + K_i^n) \tag{3}$$

where δI_{max} is the maximal current without the inhibiting ion (sodium or calcium) and K_i is the ion concentration that gives half-maximal current.

Equations for a sequential ion binding scheme were also used as follows,

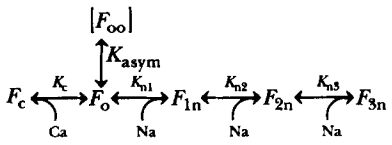

(Scheme 1)

where F_c is the fraction of binding sites with bound calcium, F_o is the fraction with no bound ion, F_{1n} is the fraction with one bound sodium ion, F_{2n} is the fraction with two bound sodium

ions, F_{3n} is the fraction with three bound sodium ions, and the constants K_c, K_{n1}, K_{n2}, and K_{n3} are the dissociation constants for the individual binding reactions. The assumption of an F_{oo} fraction, connected as indicated to the empty state (F_o), is used only in the exchange cycle simulation employed in Fig. 18 for the extracellular side. This gives one additional parameter in the denominator of the following equation, K_{asym}, which results in a lower apparent affinity of the calcium binding and the first sodium binding reaction. This is one simple way to account for lower apparent ion affinities on the extracellular side:

$$F_{3n} = [n^3/(K_{n1} \times K_{n2} \times K_{n3})]/D \tag{4}$$

$$F_c = (c/K_c)/D \tag{5}$$

where

$$D = 1 + K_{asym} + c/K_c + n/K_{n1} + n^2/(K_{n1} \times K_{n2}) + n^3/(K_{n1} \times K_{n2} \times K_{n3}) \tag{6}$$

and c and n are the free concentrations of calcium and sodium. Except for the extracellular ion binding reactions used in the simulation in Fig. 18, K_{asym} was 0. In this paper, Eq. 4 was used to

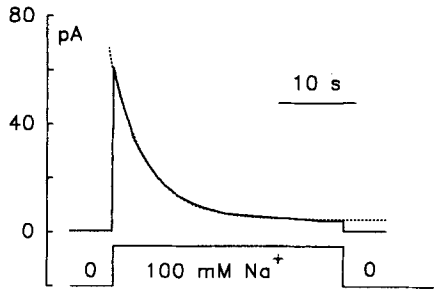

FIGURE 4. Outward sodium-calcium exchange current transient. The outward exchange current was activated by superfusion of 100 mM sodium in the presence of 2 μM cytoplasmic calcium, no extracellular sodium, and 5 mM extracellular calcium. The dotted line is a fitted single exponential (τ = 4.4 s).

fit the cytoplasmic sodium dependence of outward exchange current. Eq. 5 was used to fit the inhibition of inward exchange current by cytoplasmic sodium, where the K_c was taken from the calcium dependence of the inward current, as presented in Results.

RESULTS

Physical Factors Affecting Sodium-dependent Inactivation

Fig. 4 shows a typical outward exchange current transient obtained during application of 100 mM cytoplasmic sodium in the presence of 2 μM free cytoplasmic calcium (pipette solution A). The dotted curve is a single exponential (τ = 4.4 s) fitted to the record by a least-squares method. In the great majority of records, decay of current during application of cytoplasmic sodium was fit well (i.e., as here) by a single exponential. Apart from cases of instability, exceptions were usually cases where the inactivation had been strongly reduced by strong activators of the outward exchange current (e.g., high cytoplasmic calcium, MgATP, and chymotrypsin [Hilgemann, 1990; Collins et al., 1992] and phosphatidylserine [Hilgemann and Collins, 1992]).

As shown in Fig. 5, the selection of experimental temperature is a strong determinant of the outward current and the inactivation process. Fig. 5 *A* shows the semilogarithmic plot of the outward exchange current during application of 100 mM sodium and 1 μM calcium from a patch at 32 and 24°C (pipette solution A). An increase in temperature markedly augmented peak current and increased the rate and fractional extent inactivation. Dotted lines are fitted single exponentials (rate constants, 0.16 s^{-1} at 24°C and 0.39 s^{-1} at 32°C). Rate constants of the inactivation (●) and peak current amplitudes (○) over a wider range of temperatures are plotted semi-logarithmically in Fig. 5 *B*. The Q_{10} values for both peak exchange current and

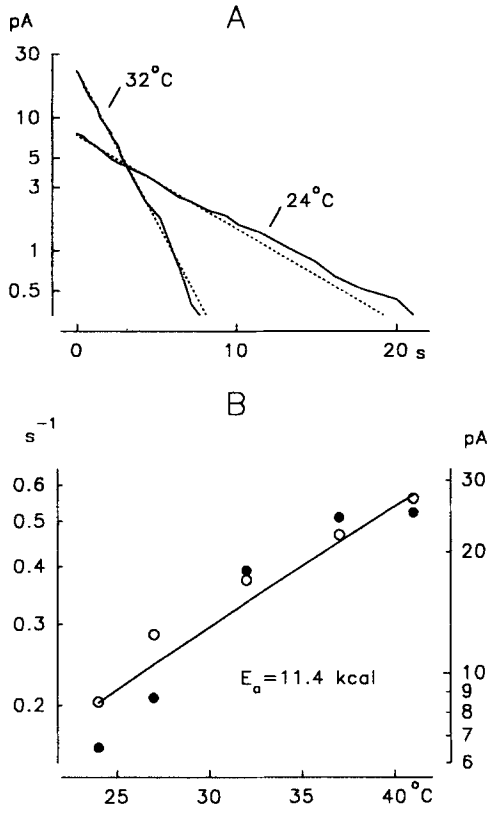

FIGURE 5. The effect of temperature on the outward exchange current. (*A*) Semilogarithmic plot of outward exchange currents during application of 100 mM sodium in the presence of 1 μM cytoplasmic calcium, no extracellular sodium, and 5 mM extracellular calcium. The two records are 24 and 32°C, as indicated, and dotted lines are single exponential plots fitted to the transients. The rate constants are 0.16 and 0.39 s^{-1} at 24 and 32°C, respectively. (*B*) Rate constant– and peak current amplitude–temperature relations. The peak exchange current (*open circles*) and the inactivation rate constants (*filled circles*) are plotted in a logarithmic scale against temperature. The line is the best fit of the inactivation rates to an Arrhenius equation. See text for details.

the rate of inactivation are 2.2. Data for the rate constants were fitted with the Arrhenius equation,

$$k = A \times e^{(-E/RT)}$$

where k is a rate constant, A is a constant, and E is activation energy (solid line). According to the Arrhenius equation, the inactivation process has an activation energy of 11.4 kcal/mol.

A second major experimental determinant of the inactivation process is the pH of cytoplasmic solutions. To examine the effect of pH, the proton-independent calcium

buffer, dibromo-BAPTA (K_d, 1.6 μM; Molecular Probes Inc.), was used as a cesium salt. For the purposes of this study, the lower affinity of this BAPTA derivative versus BAPTA itself is advantageous to allow free calcium buffering into the range of several micromolar. As shown in Fig. 6 *A* (4 μM free cytoplasmic calcium; pipette solution A), current decayed by ~85% at pH 6.8. The extent of decay was strongly reduced at pH 7.8, and this effect was immediately reversible. In our experience with pH, as with other interventions that reduce sodium-dependent inactivation, the peak current upon application of cytoplasmic sodium can be strongly increased or may be very little affected, as in Fig. 6. After the initial small decay phase at pH 7.8, current increased slowly over ~30 s (indicated by the broken record). This phenomenon has

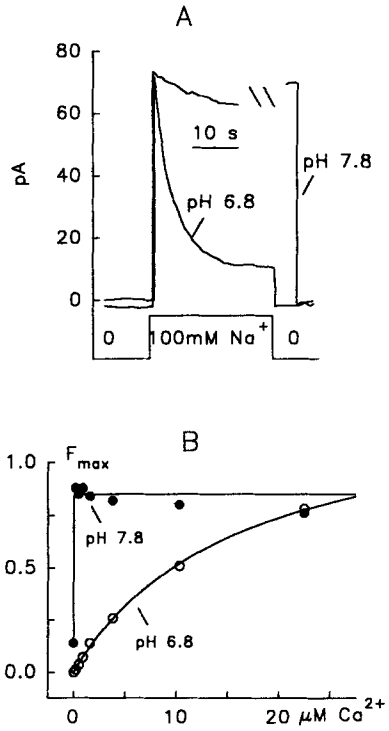

FIGURE 6. The effect of cytoplasmic pH on the sodium-dependent inactivation and on secondary activation by cytoplasmic calcium. Dibromo-BAPTA was used as calcium buffer. (*A*) Outward exchange current transient at pH 6.8 and 7.8, activated by 100 mM cytoplasmic sodium in the presence of 4 μM cytoplasmic calcium. (*B*) pH-induced shift of secondary activation by cytoplasmic calcium. Data are normalized to the fitted maximum steady-state current at pH 6.8. As indicated, open circles are at pH 6.8 and filled circles are at pH 7.8. The data at pH 6.8 are fitted with a Hill equation having a slope coefficient of 1.0 and a K_h of 9.6 μM calcium (*solid line*).

also been observed with strong activation of outward exchange current by other interventions that reduce inactivation (i.e., stimulation by MgATP and/or phosphatidylserine; unpublished observations). As shown in Fig. 6 *B*, alkalosis shifts the secondary cytoplasmic calcium dependence of outward exchange current strongly to lower free calcium concentrations. The results shown are the average of two determinations of the relationships, one experiment in which the pCa-current relation was first obtained at pH 6.8 and one in which the relation was first determined at pH 7.8. Free calcium concentrations were measured with Fura-2. The fitted K_d at pH 6.8 was 9.6 μM free calcium. The secondary activation was already maximal at 0.3 μM free calcium at pH 7.8. Accordingly, the K_d for calcium is shifted

by substantially more than 1.5 log units when pH is changed by one unit. It was noteworthy in these experiments (not presented) that at very high cytoplasmic pH values (8.8) the secondary dependence of outward exchange current on cytoplasmic calcium could be entirely lost. Similar results have been obtained using EGTA as the calcium buffer.

Inactivation Does Not Change the Voltage Dependence of the Exchanger

If the inactivation process reflects a transition of part of the total exchanger population from a fully active state to a fully inactive state, then basic properties of the exchange process should not change during the build-up of inactivation. As a first test of this prediction, *I-V* relations were determined during inactivation. Results in Fig. 7 are with pipette solution A with 2 mM extracellular calcium. Fig. 7 *A* shows the

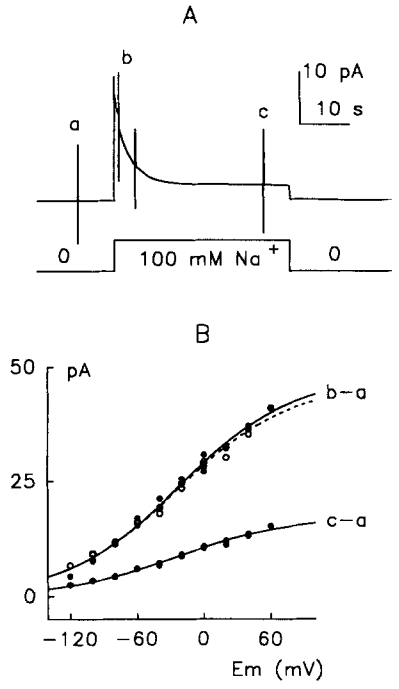

FIGURE 7. Voltage dependence of outward exchange current during sodium-dependent inactivation. (*A*) A chart record of membrane current. The outward exchange current is activated by application of 100 mM cytoplasmic sodium in the presence of 2 mM extracellular calcium and 2 μM cytoplasmic free calcium. *I-V* relations were measured before (*a*) and during (*b* and *c*) the inactivation. (*B*) *I-V* relations of the outward exchange current during inactivation ($b - a$) and at steady state ($c - a$). Open circles and a dotted curve are a scaled-up steady-state *I-V* relation ($c - a$).

usual protocol carried out. *I-V* relations were determined as indicated before application of sodium (*a*), during the early phase of inactivation (*b*), and after achieving steady-state current (*c*). Fig. 7 *B* shows the indicated subtractions, $b - a$ being early during inactivation and $c - a$ being the steady-state current. The dotted curve with open circles is a scale-up of the steady-state *I-V* relation. In this experiment, as in five similar experiments, the *I-V* relation showed no obvious change of shape. This result also negates a possibility of sodium and calcium concentration changes in both bath and pipette during the operation of the exchanger, which was the case in whole cell experiments (Kimura, Miyamae, and Noma, 1987; Ehara, Matsuoka, and Noma, 1989). It is noted that with low

extracellular calcium concentrations (0.1–0.2 mM), some flattening of the *I-V* relation during the inactivation was sometimes observed (three observations not presented). Under these conditions, depletion of the pipette calcium concentration could be significant, and reduction of extracellular calcium is known to flatten the *I-V* relation (Hilgemann, Nicoll, and Philipson, 1991*b*; Matsuoka and Hilgemann, 1992).

Similar *I-V* measurements of outward exchange current (>20 patches) were performed during secondary current changes caused by changes of cytoplasmic free calcium, by chymotrypsin, and by MgATP. No consistent changes of the *I-V* shape were observed. Fig. 8 shows a typical example of the results for cytoplasmic calcium

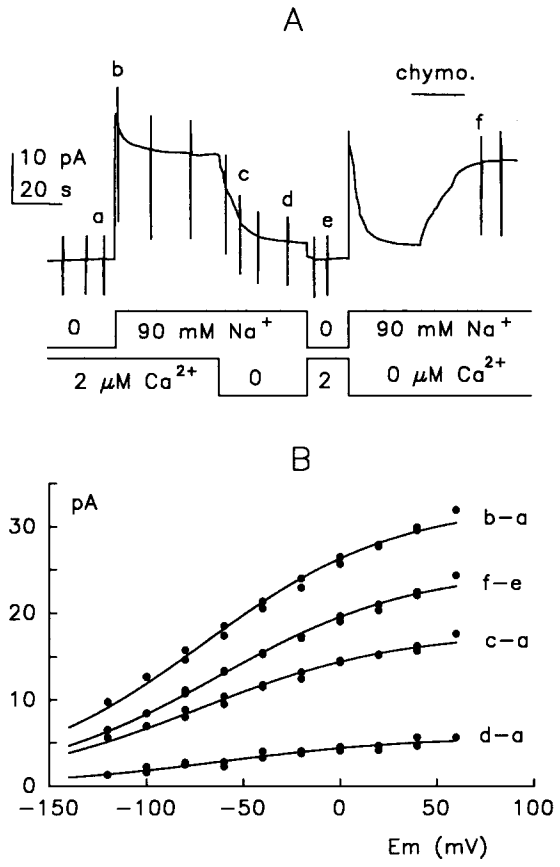

FIGURE 8. Voltage dependence of the outward exchange current during removal of cytoplasmic calcium and after treatment with chymotrypsin; 2 μM cytoplasmic calcium, no extracellular sodium, and 2 mM extracellular calcium. (*A*) The outward exchange current was activated by 90 mM cytoplasmic sodium and then cytoplasmic calcium was removed. The current was again evoked by cytoplasmic sodium without cytoplasmic calcium and finally activated by 2 mg/ml chymotrypsin (*chymo.*) as indicated. (*B*) *I-V* relations of the outward exchange current just after the application of sodium ($b - a$), during the removal of calcium ($c - a$, $d - a$), and after treatment with chymotrypsin ($f - e$). The same smoothing function multiplied by different scalers (*solid curves*) accurately describes all of the *I-V* relations.

and chymotrypsin (pipette solution A with 2 mM calcium). Results are from a patch with relatively little inactivation at 2 μM free cytoplasmic free calcium. As indicated, *I-V* relations were determined before (*a*) and just after application of 90 mM sodium (*b*), during the fall of current upon removal of cytoplasmic calcium (*c* and *d*), after removal of sodium (*e*), and after treatment with 2 mg/ml chymotrypsin in the absence of cytoplasmic calcium (*f*). As shown in Fig. 8 *B*, all of the *I-V* relations were well fit by scaling the same function up or down. Note the tendency of *I-V* relations both here and in Fig. 7 to saturate at positive potentials.

Inward and Outward Exchange Currents Are Inactivated Equally

Fig. 9 shows typical exchange current transients obtained with both sodium (150 mM) and calcium (2 mM) in the pipette (pipette solution B). Cytoplasmic free calcium was set to 1 μM. Accordingly, either inward or outward exchange current can be activated with appropriately chosen cytoplasmic solutions. The current record begins with superfusion of 1 μM free calcium and no cytoplasmic sodium. The steady-state current is −8.5 pA inward current. As indicated, 100 mM cytoplasmic sodium was then applied in the presence of the 1 μM cytoplasmic free calcium, just as in previous measurements of the outward exchange current. The current transient is very similar to records obtained without sodium in the pipette, where the steady-state outward current in the presence of 100 mM sodium is 4 pA. Next, cytoplasmic sodium was removed. The current falls into the inward current range, but it does not return immediately to the baseline level. The rapid current change terminates at −3

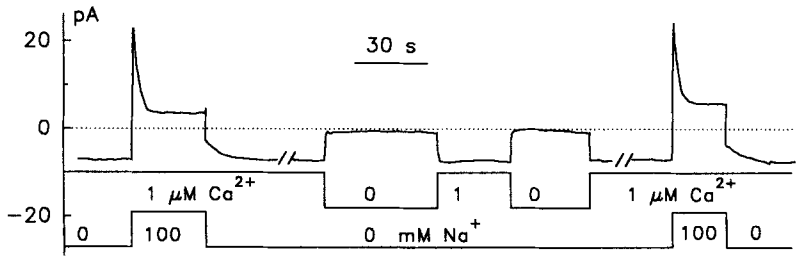

FIGURE 9. Inward and outward exchange currents with 150 mM sodium- and 2 mM calcium-containing pipette solution (pipette solution B). 100 mM sodium was first applied and removed in the presence of the 1 μM cytoplasmic calcium. Note the slow return of current to baseline upon removal of cytoplasmic sodium. Sodium-free cytoplasmic solutions were then switched between a calcium-free and a 1 μM calcium-containing solution. Note the immediate fall of inward current upon removal of calcium and the immediate increment upon reintroduction of calcium. Finally, the outward exchange current was again activated with 100 mM sodium in the presence of 1 μM cytoplasmic calcium.

pA, and it is followed by a slow equilibration phase to the baseline level with a time constant of ~6 s. This is somewhat slower than the rate of inactivation upon application of sodium, and the slow phase would logically reflect recovery from the sodium-dependent inactivation.

Next in the record in Fig. 9, cytoplasmic calcium was removed and reapplied twice. Current falls upon removal of cytoplasmic calcium within the time scale of the solution switch to nearly 0 pA. No obvious inactivation of the inward current upon application of 1 μM cytoplasmic calcium was observed. Regarding the small leak current, it is first pointed out that there is almost no monovalent ion gradient with the solutions used and, second, that the seal resistance was just 10 GΩ. The inward current activated by application of 1 μM calcium is ~8 pA in this experiment, and it was more than doubled with application of a solution with 5 μM free calcium (data not shown for brevity). Current activation upon application of calcium also took place within the time scale of the solution change. Finally, in Fig. 9, outward current was

again activated with 100 mM cytoplasmic sodium and turned off, as before, with a slow tail of increasing inward current upon removal of cytoplasmic sodium.

The mean current value obtained with the no-sodium/no-calcium cytoplasmic solution is −0.3 pA, which must be the zero exchange current level. Accordingly, outward current decay during application of sodium corresponds to 74% of peak current in the first transient and 65% of peak outward current in the transient at the end of the record. The recovering component of inward current after removal of sodium corresponds to 60 and 55% of total inward current. Thus, the percentage inactivation in 100 mM sodium, deduced separately from the outward and inward current records, is discrepant by ~15%. A possible basis for the discrepancy is that cesium is used as the sodium substitute to define outward current. Cesium generates a somewhat (~25%) larger leak current than sodium due to its higher mobility, which can lead to a small underestimation of outward current in the presence of high sodium.

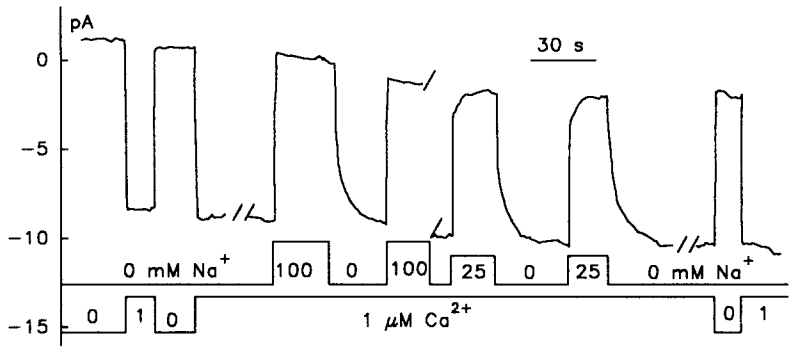

FIGURE 10. Inward sodium-calcium exchange current with calcium-free, 140 mM sodium-containing pipette solution (solution C). Inward sodium-calcium exchange current was activated twice by superfusion with 1 μM calcium-containing solution in the first part of the record. 100 mM sodium was then applied in the presence of 1 μM calcium. The inward current is immediately reduced to the zero calcium level, but recovery upon removal of sodium takes place largely with a slow time course. Next, 25 mM sodium was applied twice in the presence of 1 μM calcium. The inward current is reduced almost to the baseline level with a small, slow phase of final current inhibition. Recovery takes place with a prominent slow phase. Finally, inward current was again turned off by calcium removal and reactivated with calcium.

Sodium-dependent Inactivation of Isolated Inward Exchange Current

Fig. 10 describes sodium-dependent inactivation of the isolated inward exchange current when activated in the absence of extracellular calcium (pipette solution C). The currents described are entirely dependent on the presence of sodium in the pipette, controls having been performed with NMG, cesium, and lithium substitutions (see Fig. 3). Also, the inward exchange currents were absent when 10 mM cobalt, but no EGTA, was included in the pipette (> 10 observations).

Fig. 10 shows typical current records with inward current activation by 1 μM cytoplasmic calcium. In the absence of cytoplasmic calcium, baseline current is near zero, and in the course of this experiment the baseline drifted inward by ~1.5 pA. As

indicated in the first portion of the record, cytoplasmic calcium was applied, removed, and applied again, with activation of ~8 pA inward current within the solution switch time. Next in the record, 100 mM sodium was applied with substitution for cesium. The inward current is immediately inhibited to just the previous current baseline. Upon removal of cytoplasmic sodium, the current recovers in two phases, with the slow phase being more prominent here and having a time constant of a few seconds. Next in the record, the inhibitory effect of 25 mM sodium was tested. As apparent in the record, 25 mM sodium was enough to inhibit the current by >90% in this patch. Note a small phase of slow inhibition of the current during application of 25 mM sodium. Presumably, the inhibition by sodium reflects both direct inhibition through competition for binding sites with calcium and slow inhibition (or inactivation) as described for the outward current. In the last portion of Fig. 10, superfusion solution was again switched to a zero calcium solution and back to 1 μM free calcium to test for stability of the current.

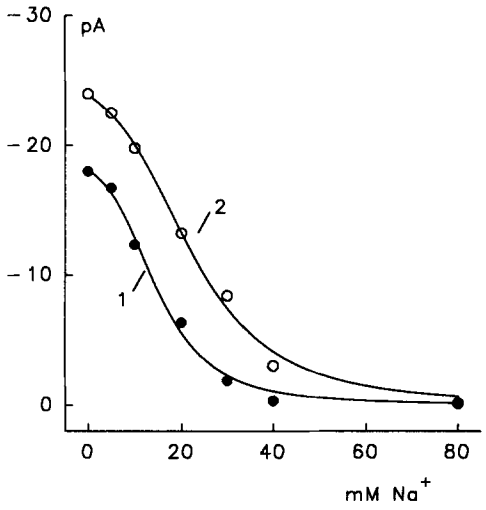

FIGURE 11. Cytoplasmic sodium dependence of inward exchange current. Pipette solution C. 3 μM cytoplasmic free calcium. Filled circles are before (*1*) and open circles are after (*2*) chymotrypsin treatment. See text for explanations of data fits.

Steady-State Inhibition of Inward Exchange Current by Cytoplasmic Sodium

Fig. 11 presents the steady-state inhibition of inward exchange current by cytoplasmic sodium with 3 μM free cytoplasmic calcium. Filled circles are before chymotrypsin treatment and open circles are after chymotrypsin treatment. Inhibition by cytoplasmic sodium begins shallowly and gains in steepness as sodium is increased with half-inhibition at 16 mM before chymotrypsin and at 22 mM after chymotrypsin. In this patch, as well as seven others, chymotrypsin increased the inward exchange current obtained with 27 μM free calcium in the absence of sodium.

The curves given in the figure are data fits to Eqs. 4–6 allowing variation of the K_{n1}, K_{n2}, and K_{n3} and a scaler variable. The dissociation constant for calcium binding, K_c, was taken from the fits of the calcium dependence of the current (not shown; see the accompanying article by Hilgemann, Collins, and Matsuoka [1992]). The wave form of steady-state inhibition by sodium is predicted by this ion binding scheme only if

the binding of the third sodium takes place with higher affinity than the first and second binding reactions. It is notable that this constraint was also found when the sodium dependence of outward current was fitted to the equivalent equation for the fraction of binding sites with three sodium ions bound (see subsequent figures).

Recovery from Sodium-dependent Inactivation

Fig. 12 describes the recovery from inactivation of the isolated outward exchange current (pipette solution A). To monitor the recovery, 100 mM sodium was first applied to fully activate outward exchange current. Then, after steady state was reached, sodium was replaced by cesium for a variable time period, after which sodium was reapplied (see inset). Rates of inactivation after the variable recovery period were very similar. At full recovery time, the rate constant of inactivation was

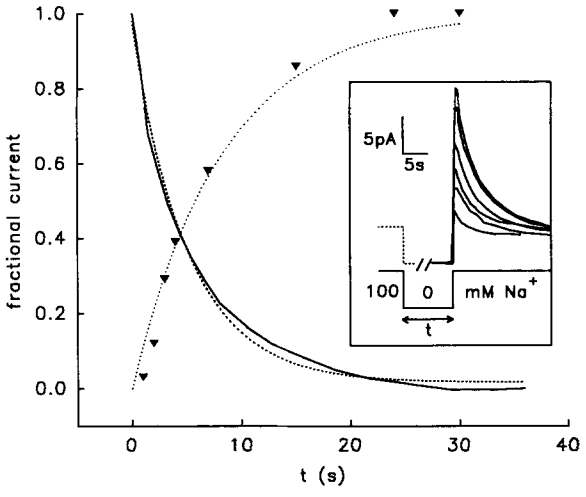

FIGURE 12. Recovery from inactivation. (*Inset*) Outward sodium-calcium exchange current was first activated by 100 mM cytoplasmic sodium, then switched off by sodium removal, and finally reactivated by 100 mM sodium after a variable recovery period (t). Current transients are superimposed at the time of reactivation. Ratios of the peak transient component currents upon a second sodium application to those upon sodium application after the longest test interval are plotted against recovery time (*filled triangles*). Data are fitted to a single exponential (ascending dotted line with a rate constant of 0.11 s^{-1}). The solid curve is a current trace during a second application of sodium after a full recovery period (>22 s), fitted to a single exponential (descending dotted line with a rate constant of 0.2 s^{-1}).

0.20 s^{-1}. Peak currents obtained upon reapplying sodium are given as triangles in Fig. 12, and a single exponential fits the data points well (dotted curve). The rate constant of recovery was 0.11 s^{-1}. It is worth noting here that in the simple case of a saturable inactivation reaction, the measured recovery rate accurately gives the rate constant of the backward reaction, while the apparent inactivation rate gives the sum of the forward and reverse reactions.

Sodium Dependence and Detailed Kinetics of Sodium-dependent Inactivation

Figs. 13 and 14 present complete cytoplasmic sodium dependencies of the outward exchange current with pipette solution A. Six experiments were performed with the same protocols. Complete sets of data were achieved in three experiments, and current run-down was smallest in the experiment selected for presentation. Shifts of

the current dependencies on sodium, apparent steepness of the sodium dependencies, and changes of the time constants of current transients described here were all verified in at least three other experiments.

As indicated in Fig. 13 *A*, cytoplasmic sodium was increased from 0 mM to a variable sodium concentration (*X*) and back to 0 mM. Then, as indicated in Fig. 13 *B*, cytoplasmic sodium was increased from a variable baseline concentration to 100 mM and back to the varied concentration. During the ~40-min experiment, a sodium concentration, *X*, was selected randomly from five chosen values. For each chosen *X*, a jump was first made to *X* from 0 mM, back to 0 mM, back to *X*, twice to 100 mM sodium from *X*, and back to *X*. Dotted lines in Fig. 13, *A* and *B*, are single exponentials, fit to the current transients by a least-squares method.

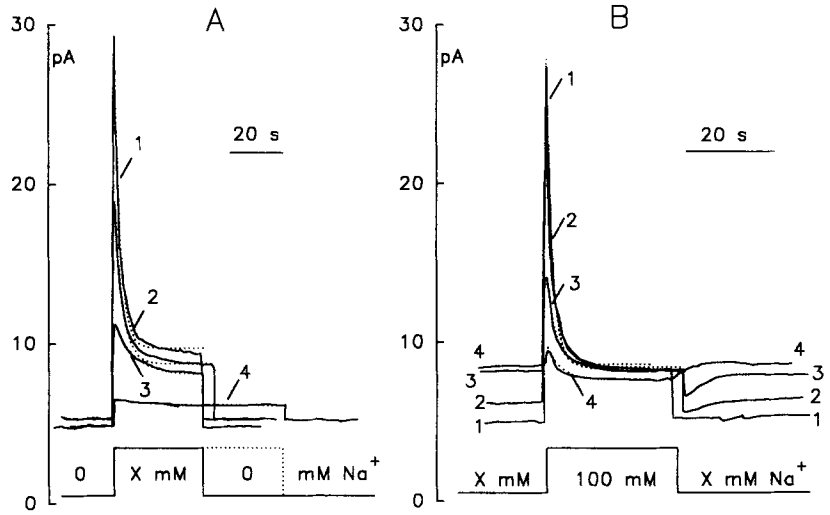

FIGURE 13. Kinetics and steady-state dependencies of outward sodium-calcium exchange current on cytoplasmic sodium. Pipette solution A, including 5 mM calcium and no sodium. (*A*) Cytoplasmic sodium was stepped from 0 mM to a variable (*X*) concentration and back to 0 mM. Curves *1–4* are to 100, 30, 16, and 8 mM, respectively. Concentration changes were made in random order. (*B*) Cytoplasmic sodium was stepped from a variable (*X*) concentration to 100 mM and back to *X* mM. Curves *1–4* are from 0, 8, 16, and 30 mM, respectively. These results were obtained in sequence with those of *A*. Dotted lines in both *A* and *B* are the best fits of single exponentials to the current transients.

Details of the results, representing averages of the available data points for the same concentration jump measurements, are presented in Fig. 14 *A*. Quasi-instantaneous sodium dependencies of the current are given as circles. Filled circles are the peak current values upon stepping from 0 to *X* sodium in Fig. 13 *A*. Open circles are the current values obtained immediately upon stepping from 100 mM sodium back to *X* sodium in Fig. 13 *B*, measured from current magnitude in zero sodium. Diamonds give the steady-state current magnitude. Filled squares give the peak sodium-sensitive current magnitude obtained in Fig. 13 *B* upon stepping to 100 mM

sodium from *X* sodium (i.e., the peak current obtained minus the leak current in 0 sodium). These data points represent steady-state inactivation.

Fig. 14 *B* shows the data in a normalized format. Note that the steady-state current (f_{ss}) is shifted to the left from the peak current values (f_{act}) as is the steady-state inactivation (h_∞). Slope values for the four curves ranged from 2.2 to 2.9 in the six experiments, with the steady-state inactivation tending to be more steep than the

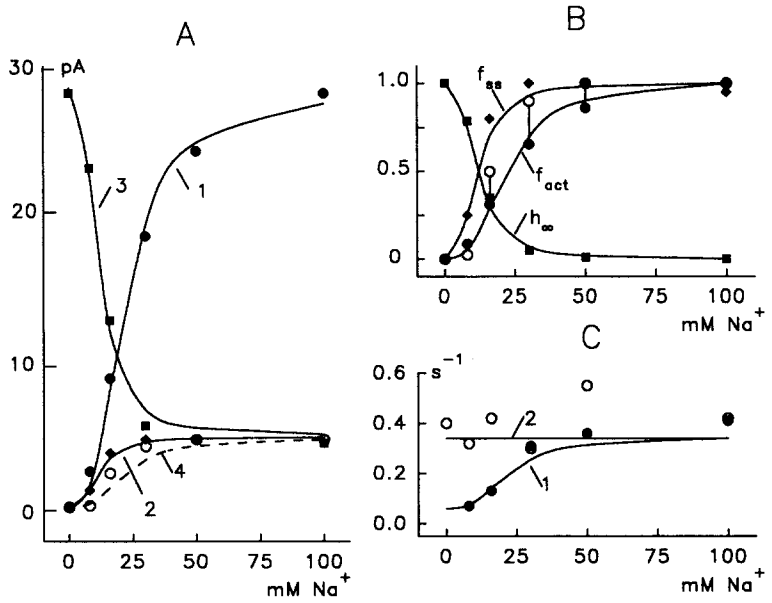

FIGURE 14. Sodium dependencies of activation and inactivation of the outward sodium-calcium exchange current. Data are from Fig. 13. (*A*) Sodium dependence of peak outward exchange current from Fig. 13 *A* (*filled circles*), sodium dependence of steady-state exchange current (*filled diamonds*), sodium dependence of steady-state inactivation from Fig. 13 *B* (*filled squares*), and sodium dependence of exchange current immediately upon switching from 100 mM in Fig. 13 *B* (*open circles*). Curves *1–4* are predicted relationships from the simple inactivation model described in the text. (*B*) Normalized data from *A*. Same symbols. Note that the normalized peak current values (*filled circles*) are not superimposed with the normalized values upon switching from 100 mM to a variable low sodium concentration (*open circles*); they are connected by vertical lines. Curves are also normalized from *A*. (*C*) Rate constants of current decay from *A* (*filled circles*) and *B* (*open circles*) in Fig. 13. All solid curves are the expected relationships for a simple inactivation model. Parameters from Scheme 1 and Eqs. 7–12 were as follows: K_{n1} = 66.8 mM, K_{n2} = 66.8 mM, K_{n3} = 1.81 mM, k_{inact} = 0.293 s^{-1}, k_{bak} = 0.0595 s^{-1}, and S = 28.50. See text for further details.

other relationships. If, for example, binding of only one sodium ion were necessary for inactivation, the Hill slope of steady-state inactivation would presumably be 1.

Fig. 14 *C* gives the rate constants of the exponentials fitted to the data in Fig. 13. Filled circles give the rate constants in dependence on the sodium concentration to which the sodium jump was made (Fig. 13 *A*). Open circles give the rate constant

dependency, or rather the lack thereof, on the sodium concentration from which the sodium jump was made to 100 mM (Fig. 13 *B*).

This data set has been fit to a simple two-state inactivation model, and results are given by the solid lines in Fig. 14. The data fit assumes that both the outward exchange current and the transition to an inactive state are directly related to the fraction of total exchanger with three bound cytoplasmic sodium ions. Recovery from the inactive state is assumed to be a simple time-dependent process. Accordingly,

$$dF_a/dt = (1 - F_a) \times k_{bak} - F_a \times F_{3n} \times k_{inact} \quad (7)$$

where F_a is the fraction of total exchanger in the active state, k_{bak} is the rate constant of recovery from inactivation, F_{3n} is the fraction of total exchanger with three bound sodium ions at cytoplasmic-facing binding sites, and k_{inact} is the rate constant of inactivation. In steady state,

$$F_a = k_{bak}/(k_{bak} + F_{3n} \times k_{inact}) \quad (8)$$

and the exchange current in steady state (I_{naca}) will be

$$I_{naca} = S \times F_a \times F_{3n} \quad (9)$$

where S is a scaler. The specific function used for F_{3n} is unimportant for this simulation, except that it must fit the quasi-instantaneous sodium–exchange current relations. For the results presented, Eqs. 4–6 for sequential binding of three sodium assumed a K_c of 2 μM.

When this equation was fit to sodium concentration–current relations for the outward exchange current (>20 data fits), the curve fitting consistently converged to a solution with the first two binding sites having low affinity and the last binding site having high affinity. For simplicity, therefore, the first two binding sites were assigned the same affinity ($K_{n1} = K_{n2}$) and one parameter was eliminated in the fitting routine.

Assuming for simplicity that all exchangers become available in the absence of sodium, the peak currents from Fig. 14 *A* (filled circles) are given by

$$I_{naca} = S \times F_{3n} \quad (10)$$

The steady-state exchange current availability (peak exchange current magnitudes in Fig. 13 *B*; squares in Fig. 14 *A*) is

$$I_{naca} = S \times F_a \quad (11)$$

The rate constants of the exponential fits in Fig. 13, *A* and *B*, plotted in Fig. 14 *C*, are

$$k_{Inaca} = k_{bak} + F_{3n} \times k_{inact} \quad (12)$$

Eqs. 7–12 were fit simultaneously to the data set, and results are given in the legend to Fig. 14. The simple inactivation model predicts very well the shift to the left of the steady-state sodium–current relation from the peak current magnitudes. Also, it predicts well that steady-state inactivation and steady-state exchange current have the same sodium dependence.

From this experiment and from three others, however, one deviation of the results from the simple model might be significant. The quasi-instantaneous sodium dependence of exchange current immediately upon application of sodium (filled

circles in Fig. 14, *A* and *B*) and after inactivation (open circles in Fig. 14, *A* and *B*) are somewhat shifted from one another. The open and closed circles are connected by a vertical line in Fig. 14 *B* to point out the discrepancy. It is noted, however, that the steady-state currents are rather small when inactivation is large, and the current measured upon reducing sodium from 100 to *X* mM sodium is related to zero current in either previous or later measurements with zero sodium (see Fig. 13 *B*). Therefore, these measurements are prone to more error than the others.

Sodium-dependent Inactivation Is Largely Voltage Independent

From these and similar experiments it is concluded that the sodium-dependent inactivation process depends on binding sites being fully loaded with sodium on the cytoplasmic side. The h_∞ curve is just as steep as the activation curve for cytoplasmic sodium. The next question, then, is how much further the cycle must or may proceed to allow the inactivation process to take place. Accordingly, variables were changed which can be expected to favor different conformations of the cycle, assuming that a consecutive-type exchange model, as provisionally suggested by Hilgemann et al. (1991*b*), is applicable to the regulated exchange system.

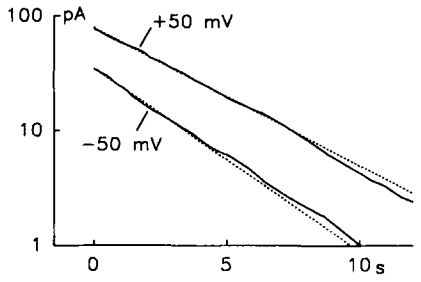

FIGURE 15. Voltage independence of sodium-dependent inactivation in guinea pig sarcolemma. Membrane currents during applications of 100 mM cytoplasmic sodium at holding potentials of +50 and −50 mV are plotted in a semilogarithmic scale after subtraction of an asymptote. Dotted lines are single exponential fits of data. Rate constants are 0.28 s^{-1} at +50 mV and 0.37 s^{-1} at −50 mV.

The first variable of interest was membrane voltage. In six experiments, the inactivation rate and the fractional inactivation during application of 100 mM cytoplasmic sodium were determined at different membrane potentials. As illustrated in Fig. 15, variation of potential by 100 mV in guinea pig sarcolemma had very little effect on the decay rate. In this case, the rate of inactivation was decreased slightly at +50 mV versus −50 mV. Correspondingly, we found little or no effect of potential on the fraction of current that inactivated in guinea pig sarcolemma. We stress, however, that there appears to be a species dependence of results on this issue. In patches from rabbit sarcolemma, both the inactivation rate and the fraction of current that inactivated increased markedly (factor 2 to 3) with a 100-mV depolarization (potential range studied, −80 to +40 mV; four observations; no data presented for brevity).

Extracellular Calcium Enhances Sodium-dependent Inactivation

A second major variable was extracellular calcium. A reduction of extracellular calcium is predicted to result in a larger fraction of exchanger binding sites being

oriented to the extracellular side and therefore not available to undergo inactivation. When experiments with both guinea pig and rabbit sarcolemmal patches were performed (>10 observations) with different extracellular calcium concentrations, both the degree of inactivation obtained and the rate of inactivation were strikingly less pronounced with low extracellular calcium (<0.5 mM) than with high extracellular calcium (>2 mM). As shown in Fig. 16 *A*, these conclusions were quantified in experiments with pipette perfusion, allowing calcium concentration changes within single experiments.

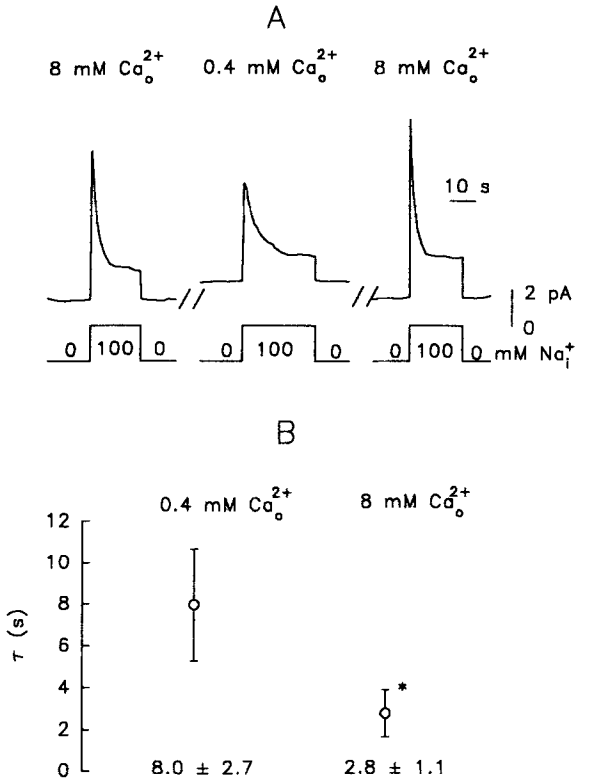

FIGURE 16. Extracellular calcium dependence of sodium-dependent inactivation. (*A*) Outward currents were induced by 100 mM cytoplasmic sodium. No extracellular sodium and 1 μM cytoplasmic calcium. Extracellular calcium was changed from 8 to 0.4 mM, and again to 8 mM with the pipette perfusion method. (*B*) Comparison of time constants (τ) of the inactivation at 0.4 and 8 mM extracellular calcium. τ = 8.0 ± 2.7 s (mean ± SD, n = 9) at 0.4 mM calcium. τ = 2.8 ± 1.1 s (n = 10) at 8 mM calcium. *P < 0.01, t test.

With 0.4 mM extracellular calcium the inactivation was less in extent and in rate. Note the complete reversibility of the transient form upon reducing calcium and then reapplying 8 mM calcium. As shown in Fig. 16 *B*, the time constant decreased significantly (P < 0.01), on average from 8.0 to 2.8 s on increasing calcium from 0.4 to 8 mM.

Simulation of Sodium-Calcium Exchange Current Transients

Our hypothesis that the inactivation process is directly related to the exchanger conformation with three bound cytoplasmic sodium ions ($E_1 \cdot 3N_i$) is further tested by a model simulation of the exchange current. A consecutive ion binding model with sodium- and calcium-occluded states reasonably described many characteristics of the

sodium-calcium exchange current (Hilgemann et al., 1991*b*). We used this model to reconstruct the sodium-calcium exchange current. Fig. 17 shows a diagram of the model. Cytoplasmic and extracellular sodium (N_i, N_o) and calcium (C_i, C_o) binding are assumed to be instantaneous. Since the rate constants for the inactivation process are many log units smaller than those for translocation steps, the inactivation step is assumed to be the only time-dependent process on a time scale of seconds.

As demonstrated in Fig. 18, this simple inactivation–activation model can describe experimental data remarkably well. Fig. 18*A* shows the inactivation of outward exchange current, whereby the outward current decays appropriately in rate and

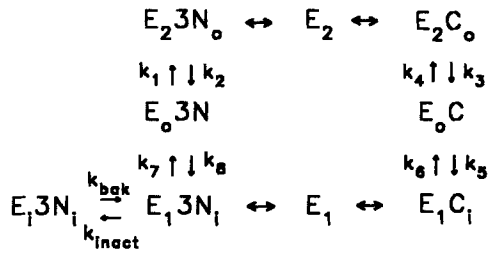

FIGURE 17. State diagram of hypothetical sodium-calcium exchange cycle. States with binding sites oriented to the cytoplasmic and extracellular sides are designated E_1 and E_2, respectively. Transitional states with occluded ions are designated E_0. Sodium and calcium binding reactions are treated as instantaneous reactions within the E_1 and E_2 states. The sodium-loaded carrier bears one positive charge. The transition between $E_2 3N_0$ and $E_0 3N$ is the single voltage-dependent step. Rate constants (s^{-1}) used for the transitions between the four exchange cycle states (E_1, E_2, E_0C, and $E_0 3N$) and the inactive state ($E_i 3N_i$) were as follows: $k_1 = 10^4 \times Kem$, $k_2 = F_{3no} \times 10^4/Kem$, where $Kem = e^{0.5 \times (1-\gamma) \times Em \times F/RT}$ and $\gamma = 0.02$, $k_3 = F_{co} \times 5.17 \times 10^4$, $k_4 = 5.17 \times 10^4$, $k_5 = 5.17 \times 10^4$, $k_6 = F_{ci} \times 5.17 \times 10^4$, $k_7 = F_{3ni} \times 1.84 \times 10^4$, $k_8 = 1.84 \times 10^4$, $k_{bak} = 0.12$, and $k_{inact} = 0.8$. The dissociation constants (mM) for calcium (K_c) and sodium (K_{n1}, K_{n2}, K_{n3}) for Scheme 1 are 0.031, 32.2, 11.1, and 11.9, respectively. On the extracellular side, $K_{asym} = 328$ (see description of Eq. 4). Also on the extracellular side, the simulated ion concentrations were modified by an assumed effect of a small narrow access channel, where the effective sodium concentration was $Na_o \times e^{-(\gamma \cdot Em \cdot F/RT)}$ and the effective calcium concentration was $Ca_o \times e^{-(\gamma \cdot 2 \cdot Em \cdot F/RT)}$. These are the same simulation scheme and parameters used in Hilgemann et al. (1991*b*). An explicit solution of the four-state model is given in Hilgemann (1988; p. 15, Routine 1). As discussed in an accompanying article (Matsuoka and Hilgemann, 1992), simulations using this scheme can be improved in reproducing *I-V* relations of exchange current in guinea pig cardiac membrane if ~12% of the voltage dependence is removed from the occlusion/deocclusion of extracellular sodium at the extracellular side (k_1–k_2 rates) and is placed on the occlusion/deocclusion of calcium from the cytoplasmic side (k_6–k_5 rates).

extent upon application of high cytoplasmic sodium. The inactivation becomes slower at low cytoplasmic sodium or extracellular calcium concentrations (second and third results in Fig. 18*A*), as shown experimentally in Figs. 13 and 16. Inward current does not decay upon an increase in cytoplasmic calcium, but recovers from the sodium-dependent inactivation with a slow time course (Fig. 18*B*). These results correspond to those of Fig. 10. In the presence of both extracellular sodium and calcium, outward current decays on application of cytoplasmic sodium and inward current increases slowly on removal of cytoplasmic sodium (Fig. 18*C*), corresponding to the results in Fig. 9. Changes of membrane potential had little or no effect on the rate or extent of inactivation (simulations not shown).

DISCUSSION

In the Introduction, the inactivation of sodium-calcium exchange current in response to high cytoplasmic sodium concentrations was compared to the analogous gating reactions of channels. This study strongly supports the idea that the inactivation process may be analyzed in terms of active and inactive exchanger states.

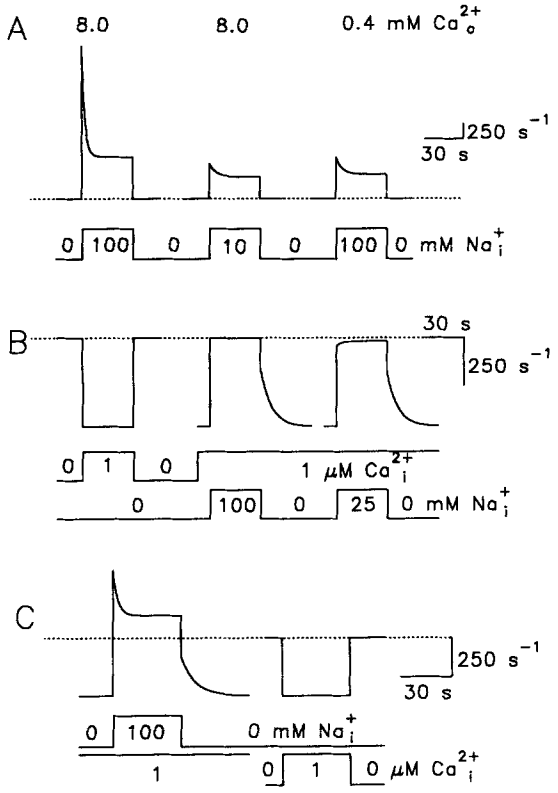

FIGURE 18. Simulation of the sodium-dependent inactivation of sodium-calcium exchange current. (*A*) Cytoplasmic sodium (Na_i^+) and extracellular calcium (Ca_o^{2+}) dependence of the inactivation of outward exchange current. Extracellular sodium (Na_o^+) is 0 mM and Ca_o^{2+} is 8 or 0.4 mM. Cytoplasmic calcium (Ca_i^{2+}) is 1 μM. (*B*) The inactivation of inward current. Na_o^+ = 150 mM. (*C*) The inactivation of mixed exchange current. Na_o^+ = 150 mM. Ca_o^{2+} = 2 mM. Dashed lines are the zero current level.

Evidence That Inactivation Takes Place from the Fully Sodium-loaded E_1 Exchanger

Multiple observations lead us to conclude that the sodium-dependent inactivation of exchange current may be specifically related to a conformation of the exchanger with binding sites oriented to the cytoplasmic side and fully loaded with sodium. In the course of our experimental analysis many alternatives were eliminated. As a first constraint, the inactivation is clearly not a general consequence of exchange activity. The isolated inward exchange current does not inactivate when activated by cytoplasmic calcium. Assuming that the exchange cycle is consecutive, this simple finding also eliminated the possibility that inactivation takes place from E_2 states with binding sites oriented to the extracellular side. Accordingly, it could be concluded that the critical steps leading to inactivation must lie between sodium binding on the

cytoplasmic side and the appearance of sodium with binding sites on the extracellular side.

That the entrance point to the inactive state takes place from a state that is a fully sodium-loaded state, probably with cytoplasmic-oriented binding sites ($E_1 3N_i$) is favored by four findings. First, the steady-state inactivation of exchange current (Fig. 14) has a dependence on cytoplasmic sodium that is at least as steep as the exchange current itself. Thus, multiple sodium ions, presumably the same number as required for transport, must bind to allow inactivation. Second, a reduction of extracellular calcium markedly decreases the rate and extent of inactivation. In a consecutive-type exchange model, reduction of extracellular calcium will allow more exchangers to orient to the extracellular side, thereby decreasing the availability of exchangers with cytoplasmic-oriented binding sites. Accordingly, exchanger availability for the inactivation reaction is reduced. Third, the fact that depolarization does not enhance inactivation must indicate that inactivation takes place from a state affected only slightly by voltage. This is the case for the $E_1 3N_i$ state in the simulated model because this state is separated from the voltage-dependent transition by at least one voltage-independent transition in each direction. Fourth, with outside-out patches, application of sodium to the extracellular membrane face (i.e., in the bath solution) in the absence of sodium in the pipette (i.e., at the cytoplasmic membrane face) induced large inward exchange currents that did not decay (routine unpublished observations; one result from an outside-out patch is presented in the accompanying article by Matsuoka and Hilgemann [1992]). This result indicates that loading of binding sites with sodium at the extracellular side does not support inactivation.

The model used for Fig. 18 obeys all requirements to account for our observations on inactivation. In the exchange model used, the voltage-dependent step is separated by at least one time-dependent step in each direction from the $E_1 3N_i$ state. Accordingly, voltage does not affect the availability of the $E_1 3N_i$ state. Simpler two-state models with voltage dependence placed on sodium translocation result in a loss of E_1 state exchanger with depolarization.

Sodium-dependent Inactivation as the End Point of Exchanger Modulation by Cytoplasmic Messengers

It is now evident that the sodium-dependent inactivation process is modulated by multiple factors besides cytoplasmic sodium, which are probably physiological regulators. Outward exchange current is activated by cytoplasmic calcium (Miura and Kimura, 1989), whereby the sodium-dependent inactivation is in some way attenuated (Fig. 2 of Hilgemann, 1990), and analysis of these interactions is presented in an accompanying article (Hilgemann et al., 1992). As described here in Fig. 6, the inactivation process is also highly dependent on cytoplasmic pH. A decrease in cytoplasmic protons can strongly attenuate the sodium-dependent inactivation and decrease the apparent K_d for cytoplasmic calcium without markedly changing the maximal steady-state current. This result could mean that protons compete at the secondary regulatory site for calcium over the physiological pH range. Two protons might compete with one calcium ion, since the shift in calcium dependence is greater than that expected for a one-to-one competition. A strong reservation about this

interpretation, however, is that other interventions that reduce sodium-dependent inactivation by undoubtedly noncompetitive means can substantially shift the apparent affinity for calcium in secondary exchange modulation. A major example is MgATP (DiPolo and Beaugé, 1987).

As pH was increased to 7.8, a significant outward current was activated by cytoplasmic sodium in the absence of cytoplasmic calcium. This calcium-independent component cannot be explained by simple competition, and the secondary dependence of outward exchange current on cytoplasmic calcium could be completely removed at higher pH values (unpublished observations). A. Doering and W. J. Lederer (1993) have recently reported that the action of protons in inhibiting outward exchange current is noncompetitive with cytoplasmic calcium. Importantly, they examined a more acid pH range (7.2–6.4) than we have examined, and they included MgATP in cytoplasmic solutions, which may have minimized the role of sodium-dependent inactivation. In spite of the noted differences in experimental results between their study and our observations, both sets of results indicate that protons act by at least two mechanisms different than competition for transported ions at transport binding sites.

While the possible physiological relevance of the effects of MgATP and negatively charged phospholipids on inactivation remains to be established, changes of cytoplasmic calcium, proton, and sodium concentrations can all be expected to modulate exchange function physiologically. Nevertheless, we must stress that the functional existence of sodium-dependent inactivation remains to be established in intact myocytes. Our present hypotheses about the inactivation predict that under appropriately chosen conditions equivalent exchange current transients might be obtained in intact heart cells with large step increases of cytoplasmic calcium. Optimized conditions would be (*a*) saturating cytoplasmic concentrations of sodium, (*b*) submaximal concentrations of free cytoplasmic calcium for secondary activation, and (*c*) rapid application of a high cytoplasmic calcium concentration. The metabolic status of cells is a likely fourth variable of importance.

Chymotrypsin

Chymotrypsin activates the exchanger and removes the inactivation and secondary calcium regulation (Hilgemann, 1990). If chymotrypsin abolishes inactivation taking place through the $E_1 3N_i$ state, the cytoplasmic sodium dependence of the exchange should decrease after treatment with chymotrypsin. As predicted, the cytoplasmic sodium dependence of inward exchange current (i.e., inhibition of the current) was indeed shifted to a higher concentration range after chymotrypsin treatment (Fig. 11). Assuming that the exchanger operates physiologically as a calcium efflux mechanism, the position and shape of this curve will be an important determinant of exchange function. The voltage dependence of *I-V* relations was not significantly altered by activation by chymotrypsin (Fig. 8), consistent with the idea that the major effect could be to remove exchangers from a fully inactive state rather than modifying the function of preexisting exchangers. That chymotrypsin also increased the amplitude of inward exchange current in the absence of cytoplasmic sodium is indicative of some additional functional effect of chymotrypsin treatment.

What Does the Inactivation Process Sense?

Our hypothesis naturally raises a question about the biophysical signal sensed by the inactivation process. In channels, three factors are well established. First, inactivation may sense the conformation changes of channel activation and opening. Second, inactivation may be an intrinsically voltage-dependent process. And third, ligand binding may initiate inactivation or inactivation-like reactions of the channel. In our case, what must be sensed is the full loading of ion transport sites, perhaps with analogy to the dependence of sodium pump phosphorylation on occupation of sodium binding sites in E1 configuration (e.g., Sachs, 1991). The specific transduction signal could be a conformational change per se (e.g., the same one that allows translocation reactions to occur), and/or a change of local electrical field with sodium binding. The recent identification of critical exchanger regions involved in the secondary modulatory reactions by mutagenesis studies of the cloned exchanger (Matsuoka, S., D. A. Nicoll, R. F. Reilly, D. W. Hilgemann, and K. D. Philipson, manuscript submitted for publication) bodes well for progress in understanding the molecular basis of the sodium-dependent inactivation process.

We thank Henry Liao for technical assistance and Dr. Binxian Zhang for measurements of free calcium with Fura-2.

This work was supported by NIH grant R29 HL-45240, an Established Investigatorship, and a Grant-in-Aid of the American Heart Association to D. W. Hilgemann, and by a grant from the Japan Heart Foundation to S. Matsuoka.

Original version received 29 July 1992 and accepted version received 25 September 1992.

REFERENCES

Blaustein, M. P., R. DiPolo, and J. P. Reeves. 1991. Sodium-calcium exchange: proceedings of the second international conference. *Annals of the New York Academy of Sciences.* 639:1–671.

Carafoli, E. 1991. The calcium pumping ATPase of the plasma membrane. *Annual Reviews of Physiology.* 53:531–547.

Collins, A., A. V. Somlyo, and D. W. Hilgemann. 1992. The giant cardiac membrane patch method: stimulation of outward Na^+-Ca^{2+} exchange current by MgATP. *Journal of Physiology.* 454:27–57.

DiPolo, R., and L. Beaugé. 1987. Characterization of the reverse Na/Ca exchange in squid axons and its modulation by Ca_i and ATP: Ca_i-dependent Na_i/Ca_o and Na_i/Na_o exchange modes. *Journal of General Physiology.* 90:505–525.

Doering, A., and W. J. Lederer. 1993. The mechanism by which cytoplasmic protons inhibit the sodium-calcium exchange in guinea pig heart cells. *Journal of Physiology.* In press.

Ehara, T., M. Matsuoka, and A. Noma. 1989. Measurement of reversal potential of Na^+-Ca^{2+} exchange current in single guinea-pig ventricular cells. *Journal of Physiology.* 410:227–249.

Ehara, T., A. Noma, and K. Ono. 1988. Calcium-activated non-selective cation channel in ventricular cells isolated from adult guinea-pig hearts. *Journal of Physiology.* 403:117–133.

Hilgemann, D. W. 1988. Numerical approximation of sodium-calcium exchange. *Progress in Biophysics and Molecular Biology.* 51:1–45.

Hilgemann, D. W. 1989. Giant excised cardiac sarcolemmal membrane patches: sodium and sodium-calcium exchange currents. *Pflügers Archiv.* 415:247–249.

Hilgemann, D. W. 1990. Regulation and deregulation of cardiac Na^+-Ca^{2+} exchange in giant excised sarcolemmal membrane patches. *Nature.* 344:242–245.

Hilgemann, D. W., and A. Collins. 1992. Mechanism of cardiac Na^+-Ca^{2+} exchange current stimulation by MgATP: possible involvement of aminophospholipid translocase. *Journal of Physiology.* 454:59–82.

Hilgemann, D. W., A. Collins, D. P. Cash, and G. A. Nagel. 1991*a*. Cardiac Na^+-Ca^{2+} exchange system in giant membrane patches. *Annals of the New York Academy of Sciences.* 639:126–139.

Hilgemann, D. W., M. J. Delay, and G. A. Langer. 1983. Activation-dependent cumulative depletions of extracellular free calcium in guinea pig atrium measured with antipyrylazo III and tetramethylmurexide. *Circulation Research.* 53:779–793.

Hilgemann, D. W., A. Collins, and S. Matsuoka. 1992. Steady-state and dynamic properties of cardiac sodium-calcium exchange. Secondary modulation by cytoplasmic calcium and ATP. *Journal of General Physiology.* 100:933–961.

Hilgemann, D. W., D. A. Nicoll, and K. D. Philipson. 1991*b*. Charge movement during Na^+ translocation by native and cloned cardiac Na^+/Ca^{2+} exchanger. *Nature.* 352:715–718.

Hille, B. 1992. Ionic Channels of Excitable Membranes. 2nd ed. Sinauer Associates, Inc., Sunderland, MA. 607 pp.

Kimura, J., S. Miyamae, and A. Noma. 1987. Identification of sodium-calcium exchange current in single ventricular cells of guinea-pig. *Journal of Physiology.* 384:199–222.

Läuger, P. 1991. Electrogenic Ion Pumps. Sinauer Associates, Inc., Sunderland, MA. 61–81.

Matsuoka, S., and D. W. Hilgemann. 1992. Steady-state and dynamic properties of cardiac sodium-calcium exchange. Ion and voltage dependencies of the transport cycle. *Journal of General Physiology.* 100:963–1001.

Miura, Y., and J. Kimura. 1989. Sodium-calcium exchange current. Dependence on internal Ca and Na and competitive binding of external Na and Ca. *Journal of General Physiology.* 93:1129–1145.

Niggli, E., and W. J. Lederer. 1991. Molecular operations of the sodium-calcium exchanger revealed by conformation currents. *Nature.* 349:621–624.

Sachs, J. R. 1991. Successes and failures of the Albers-Post model in predicting ion flux kinetics. *In* The Sodium Pump: Structure, Mechanism, and Regulation. J. H. Kaplan and P. DeWeer, editors. The Rockefeller University Press, New York. 249–266.

Soejima, M., and A. Noma. 1984. Mode of regulation of the ACh-sensitive K-channel by the muscarinic receptor in rabbit atrial cells. *Pflügers Archiv.* 400:424–431.

Stein, W. D. 1986. Transport and Diffusion across Cell Membranes. Academic Press, Inc., San Diego. 159–176.